Virchows Archiv
https://doi.org/10.1007/s00428-025-04219-x

ORIGINAL ARTICLE

Definition of parameters and thresholds to detect *MYCN* amplification in retinoblastomas

C. Bielefeld[1,2] · T. Hugo[2] · N. Sievers[2] · P. Ketteler[3,4] · E. Biewald[5] · T. Kiefer[5] · K. Papaioannou[4] · P. Tüller[4] · T. Ryl[4] · M. Busch[6] · J. Rawitzer[7] · H.-U. Schildhaus[2] · S. Ting[1,2]

Received: 27 May 2025 / Revised: 28 July 2025 / Accepted: 1 August 2025

Abstract

Retinoblastoma is a malignant childhood neoplasm where *MYCN* amplification defines a subset of tumors with worse prognosis. FISH (fluorescence in situ hybridization) represents a fast and reliable method to measure gene copy numbers in various tumors but has not yet been systematically evaluated in retinoblastoma. In this study, we define criteria for FISH detection of *MYCN* amplification in a systematic unbiased approach by using a well characterized series of 44 clinical retinoblastoma samples. We (i) determined potential measurements and parameters by a comprehensive literature review, (ii) analyzed a retrospective cohort of samples with known *MYCN* amplification, (iii) determined statistically measurements and cut-offs, which allow reliable detection of amplified tumors, and (iv) applied these criteria to a prospective cohort. We demonstrate that average gene copy number (AVGCN) of *MYCN*/cell, *MYCN*/CEN2 ratio, and *MYCN*-CEN2 difference reveal the lowest statistical variance in amplified samples, if at least 50 cells were counted. The combination of these three parameters and cut-offs, namely AVGCN ≥ 10, *MYCN*/CEN2 ratio ≥ 3, and *MYCN*-CEN2 difference ≥ 8, allowed a reliable distinction between amplified and non-amplified cases. The prevalence of *MYCN*-amplified cases was 4/33 (12.1%) among prospective clinical samples indicating a higher percentage of positive tumors than previously reported. Our data provide the first evidence for well-grounded *MYCN* FISH criteria in retinoblastoma.

Keywords *MYCN* amplification · Retinoblastoma · FISH · Ophthalmic pathology · Prognostic biomarker

Introduction

Retinoblastoma (RB) is a rare childhood malignancy, yet it is considered the most common eye cancer worldwide. The incidence of RB amounts approximately 7.2 per 100,000 live births in Europe [1]. Early diagnosis and rapid treatment of RB are of paramount importance for clinical outcome and overall survival. In recent years, modern multimodal therapies have dramatically improved overall survival rates of more than 95% and eye salvage rates of 70% in high-income countries, whereas the mortality rate is still high in low-income countries [2, 3]. Advanced stage of disease, especially extraocular tumor growth and metastasis, is a poor prognostic factor. A variety of classification systems exist, e.g., ICRB (Classification of Intraocular Retinoblastoma) to classify intraocular tumor growth, as well as IRSS (International Retinoblastoma Staging System) for extraocular retinoblastoma growth after enucleation [4]. These systems allow risk stratification and treatment options, which are based on the stage of the disease. Besides enucleation,

H.-U. Schildhaus and S. Ting contributed equally and share senior authorship.

✉ C. Bielefeld
bielefeld@patho-nordhessen.de

1 Reference Pathology for Pediatric Eye Tumors, Kassel, Germany

2 Institute of Pathology Nordhessen, Germaniastrasse 7, 34119 Kassel, Germany

3 German Consortium for Translational Cancer Research (DKTK), Essen, Germany

4 Department of Pediatrics 3, University Hospital Essen, University of Duisburg Essen, Essen, Germany

5 Department of Ophthalmology, University Hospital Essen, University of Duisburg Essen, Essen, Germany

6 Institute for Anatomy II, Department of Neuroanatomy, Medical Faculty, Center for Translational Neuro- and Behavioral Sciences (C-TNBS), University of Duisburg-Essen, Essen, Germany

7 Institute of Pathology, University of Duisburg-Essen, University Hospital Essen, Essen, Germany

Published online: 21 August 2025

various eye-preserving strategies have been established, including intravenous, intra-ophthalmic arterial, intravitreal, periocular, and systemic chemotherapy, different types of radiotherapy, such as external-beam radiotherapy and brachytherapy, and local consolidation therapies [2–5]. However, treatment-related toxicity and vision-threatening complications may have severe consequences, especially taking into account the young age of patients. Thus, secure and durable prognostic biomarkers are needed to avoid both under- and overtreatment.

Genetically, the majority of retinoblastomas arise from biallelic inactivating mutations [6] of the tumor suppressor gene *RB1* in a cone cell precursor of the developing retina [7–9]. Constitutional heterozygosity for a loss-of-function type variant of the *RB1* gene causes heritable predisposition to RB and is found in 40–45% of patients. Mutational inactivation of the other allele in a somatic cell initiates development of a tumor focus. Tumor development in patients with non-heritable retinoblastoma is caused by two somatic mutations, and most often, only a single tumor focus is present [8, 10–12]. Approximately 3% of non-hereditary, unilateral RB do not harbor *RB1* inactivation. However, half of these cases (approximately 1.5%) show somatic amplification of the *MYCN* gene in the tumor [7, 10, 12]. Recent studies on gene expression and methylation profiling have divided RB into two subtypes, which also differ in clinical behavior and presumably in prognosis [9, 11]. Subtype 1 includes few genetic alterations other than the initiating *RB1* inactivation and an expression of markers reflecting a cone-differentiated state. Contrarily, subtype 2 tumors express markers of less differentiated cone and are estimated to arise in an earlier stage of retinal development, harbor frequent genetic alterations including *MYCN* amplification, show distinct inter- and intratumoral heterogeneity, and behave more aggressively with higher risk for metastasis [8, 9, 11]. Accordingly, patients with *MYCN*-amplified tumors are younger at time of first diagnosis [10, 13, 14], a fact suggesting that more intensive and tailored treatment is required [9, 11]. Rushlow et al. have shown larger and advanced tumors at time of diagnosis and an average age of onset of 4.5 months in patients with *MYCN* amplification compared to 24 months in non-amplified cases [10]. Also, *MYCN*-amplified retinoblastomas often harbor an undifferentiated histological phenotype, especially enlarged nuclei with prominent nucleoli, necrosis, little calcification, and high Ki67 proliferation rate. It is noteworthy that only tissue of advanced tumors requiring enucleation of the affected eye is examined histologically, since biopsies of intraocular tumors are obsolete [9, 15, 16].

The *MYCN* proto-oncogene, a member of the MYC oncogene family, plays an important role in proliferation, apoptosis, metabolism, and differentiation of progenitor cells belonging to different organ systems, especially during neuronal development and differentiation [17–21]. *MYCN* as a transcription factor has anti-apoptotic effects and is a key player in shortening the cell cycle by promoting transition from the G1 phase to the S phase and by downregulation of cyclin-dependent kinases inhibitors, simultaneously enforcing ribosomal biogenesis and mRNA translation. Thus, deregulation of the *MYCN* signaling pathway can lead to an imbalance between uncontrolled proliferation and reduced apoptosis in tumorigenesis [12, 19, 22]. Moreover, *MYCN* is related to tumor drug resistance as it is associated with higher expression of multiple resistance protein 1 (MRP1), resulting in low intracellular drug concentration of chemotherapies and potential treatment failure [21]. Therefore, *MYCN* represents a potentially valuable direct or indirect therapeutic target currently under experimental investigation [19, 23]. For example, the inhibition of *MYCN* expression at the transcriptional or translational level could strengthen antitumor efficacy [21]. Ryl et al. have shown that *MYCN* knockdown in RB cell models can lead to growth arrest of tumor cells [9].

Besides RB, *MYCN* amplification plays an important role in a variety of other childhood malignancies, such as pleuropulmonary blastoma and Wilms tumor [22, 24], and also in cancers emerging in adulthood, e.g., prostate and lung cancer, gastric adenocarcinoma, and leukemia [19, 20, 25–27]. *MYCN* amplification can be detected in other neuroblastic tumors, such as neuroblastomas, astrocytomas, spinal ependymomas, and medulloblastomas, associated with aggressive clinical behavior and consequently worse prognosis [18, 20, 28–30]. Thus, evaluation of *MYCN* amplification has become clinically more relevant as a predictor of poor prognosis. For example, it is routinely assessed in medulloblastomas by fluorescence in situ hybridization (FISH), a method currently recognized as the gold standard procedure [17, 31].

FISH is generally a well-established, efficient, and reliable molecular technique for detecting gene amplifications. FISH has been widely adopted in clinical diagnostics due to its rapid turnaround, cost-effectiveness, and high sensitivity in identifying gene amplifications, which can serve as relevant prognostic and predictive biomarkers in various human malignancies. Despite its widespread use, the interpretation of FISH results is influenced by tumor type, clinical context, and the specific biomarker being assessed [32–40]. In clinical routine diagnostics, FISH is commonly employed to detect gene amplifications, which may serve as biomarkers for cancer prognosis or treatment response. For example, *ERBB2* amplification is a recognized biomarker in breast and gastric cancer, and FISH is the preferred method for its assessment [38–40]. However, the interpretation of amplification status requires careful standardization of criteria, which should be tailored to the gene of interest and the tumor subtype under investigation [33, 34, 36, 37].

To establish robust and reproducible FISH criteria, a comprehensive analysis of well-characterized tumor

cohorts is essential. This approach allows for an unbiased characterization of the distribution of amplification levels, enabling the definition of clear, empirically derived thresholds for amplification positivity [33].

In the case of retinoblastomas, specific and reliable criteria for assessing *MYCN* amplification using FISH have yet to be defined. This study aims to fill this gap by developing and validating FISH-based criteria for *MYCN* amplification in retinoblastomas. Using a well-characterized retrospective cohort, we have identified key parameters and established threshold values, which differentiate amplified from non-amplified cases. These criteria were then applied to a prospective validation cohort, providing preliminary data on the prevalence of *MYCN* amplification in retinoblastoma and contributing to the refinement of diagnostic and prognostic strategies for this rare pediatric malignancy.

Materials and methods

Samples

The overall study cohort consisted of 44 cases of retinoblastomas treated by enucleation. The retrospective group comprised 11 cases from patients where increased copy numbers of the *MYCN* gene locus in DNA from fresh frozen tumor samples had been detected by real-time qPCR (ΔCT values ranging from 4.76 to 39.28). Additionally, *RB1* status has been analyzed in all tumors. All retrospective cases showed mono- or biallelic *RB1* mutation. In 8 of 11 tumors, biallelic inactivation of the *RB1* gene (*RB1* -/-) was present, whereas the remaining three showed inactivation of only one allele of *RB1* (*RB1* +/-). None of the 11 cases showed proficient *RB1* status, actually a *RB1* wildtype (*RB1* +/+). The prospective cohort consisted of 33 RB cases, which have been routinely assessed as part of our referral service at the Reference Pathology Center for Pediatric Eye Tumors between July 2023 and end of June 2024. *RB1* status was available in 19/33 cases from the prospective group with biallelic RB1 loss in 15/15 non-amplified and 3/4 amplified cases. Some patients from both cohorts had undergone neoadjuvant therapies. All enucleation specimens were routinely processed, formalin-fixed, and paraffin-embedded. H&E staining and immunohistochemistry including CRX and Ki67 have been carried out as previously described [41]. The use of patients' material has been approved by the local ethics committees (Essen: 13–5405-BO [12/04/2023]; Kassel: 2024–3926-evBO [FF61/2014], Ethik-Kommission bei der Landesärztekammer Hessen).

Systematic review of literature

In order to determine potential criteria and thresholds, we performed a systematic literature search on previous publications on *MYCN* amplification using the PubMed database (https://pubmed.ncbi.nlm.nih.gov/). First, "retinoblastoma *MYCN* amplification" and "retinoblastoma *MYCN* amplification FISH" were applied as keywords. Second, to expand the search on tumor entities beyond RB, the terms "*MYCN* amplification FISH" were used. Clinical trials examining human tumor tissue for *MYCN* gain/amplification by FISH were included (Table 1). Besides FISH, other molecular pathological methods were also investigated in a part of these studies. We especially focused on studies, which additionally conducted PCR, especially qPCR, to measure *MYCN* amplification. As a requirement for a publication to be included in our research, the amount of cells counted and the FISH criteria used to define cases as positive for *MYCN* amplification had to be described. Moreover, the prevalence of *MYCN* amplification in each study for the respective tumor entity was recorded.

FISH

FFPE samples were processed using the ZytoLight FISH-Tissue Implementation Kit and the ZytoLight® SPEC *MYCN*/2q11 Dual Color Probe (Zytovision-Z-2028–5/−20, ZytoVision GmbH, Bremerhaven, Germany). The FISH protocol was performed according to previously established methods [49], with pepsin digestion used for proteolysis according to the manufacturer's recommendation. During FISH evaluation, the entire tumor area was examined to identify regions with amplification hot spots. In cases where *MYCN* signals displayed a homogeneous distribution, random areas were selected for analysis. A total of 100 tumor cell nuclei were evaluated, with 20 contiguous nuclei counted from five distinct areas, including both hot spots and randomly selected regions (resulting in 8800 individual cell counts for both, *MYCN* and CEN2). For each nucleus, the number of green *MYCN* and orange CEN2 signals was recorded. A Leica DM6B fluorescence microscope, equipped with appropriate filters and 63 × and 100 × oil immersion objectives, was used for evaluation (Leica, Wetzlar, Germany). All FISH samples have been evaluated by experienced FISH readers (CB, HUS, ST).

Statistical analysis

Data collection and analysis was performed using IBM SPSS Statistics software, Version 29.0.2.0. The number of signals for *MYCN* and CEN2 in 20, 50, and 100 tumor cells was documented for each case (264 data points from 44 cases). Based on this, median, mean, range (maximum and

Table 1 Summary of methods and criteria, which have been described in the literature for detecting *MYCN* amplification in retinoblastoma (RB) and other tumor entities

Tumor entity	Prevalence of *MYCN* amplification	Methods	Criteria for FISH positivity	Source
Retinoblastoma (RB)	33.3% (1/3; grading of amplification: "moderate")	FISH southern blot and PCR	AVCGN of *MYCN*; grading of amplification -"high": AVGCN > 50 (not countable) -"moderate": AVGCN 11–50 -"weak": AVGCN 3–10 -"not amplified": AVGCN 0–2	[41]
	2/2 cases	FISH	≥ 10% of tumor cells GCN of *MYCN* > 8 and ratio > 4	[15]
Spinal ependymoma	100% (13/13; 10 WHO grade III, 3 WHO grade II)	FISH CNVs, RNA sequencing, Affymetrix arrays	200 cells counted > 10% of tumor cells GCN of *MYCN* > 8 and ratio > 4 or > 10% of tumor cells with strong clusters	[20]
	100% (8/8; all WHO grade III)	FISH NGS (incl. PCR)	60 cells counted > 10% of tumor cells GCN of *MYCN* > 6	[42]
	9.1% (2/22)	FISH	100 cells counted ratio > 1.25 GCN of *MYCN* > 10 in > 80% of cells	[43]
Glioblastoma	8.6% (3/35)	FISH sanger sequencing (PCR), CNV analysis, targeted DNA + RNA sequencing	100 cells counted cluster formation or ratio > 2 in > 5% of tumor cells	[44]
Neuroblastoma	30.8% (24/78) -Middle East 44.1% -North America 20.5%	FISH	200 cells counted AVGCN of *MYCN* ≥ 10 and ratio ≥ 3	[45]
	32% (8/25; only "moderate" and "high")	FISH southern blot and PCR as control	AVCGN of *MYCN*; grading of amplification -"high": AVGCN > 50 (not countable) -"moderate": AVGCN 11–50 -"weak": AVGCN 3–10 -"not amplified": AVGCN 0–2	[41]
	25.8% (11/43) (10/11 with ratio > 6)	FISH	60 cells counted average ratio > 2	[46]
	32.2% (37/115)	FISH qPCR (plasma *MYCN*/NAGK ratio)	average ratio > 4	[47]
	13.5% (24/178)	FISH	200 cells counted -"amplification": difference AVGCN *MYCN*—AVGCN CEP2 ≥ 10 -"gain": difference AVGCN *MYCN*—AVGCN CEP2 1–9 -"not amplified": 2 *MYCN* and 2 CEP2 signals/cell	[48]
Ganglioneuroblastoma	Amplification 3% (1/32), "gain" 14% (25/32)			
Ganglioneuroma	Amplification 0%, "gain" 40% (4/10)			

Table 1 (continued)

Tumor entity	Prevalence of *MYCN* amplification	Methods	Criteria for FISH positivity	Source
Medulloblastoma	18.2% (4/22)	FISH qPCR	200 cells counted > 10% of tumor cells ratio > 2 or strong clusters	[18]
	6.5% (17/260)	FISH PCR	100 cells counted by two investigators > 10% of tumor cells with strong clusters or GCN of *MYCN* > 8	[30]
	10% (7/70; "amplification") 5.7% (4/70 MYC-amplification; 1 subclonal)	FISH	200 cells counted -"subclonal amplification": ≥ 10% of tumor cells with GCN of *MYCN* ≥ 10 -"amplification": ≥ 50% of tumor cells with GCN of *MYCN* ≥ 10 -"not amplified": GCN of *MYCN* ≤ 4	[31]
	34.9% (6/64)	FISH mRNA nCounter assay	100 cells counted average ratio > 2 or uncountable cluster formation or > 10% of tumor cells with GCN of *MYCN* ≥ 8	[23]
Neuroendocrine prostate cancer	Primary hormone naïve: 46.7% (7/15) treatment-related: 43.5% (20/46) metastases: 71.4% (10/14)	FISH	50 cells counted AVGCN of *MYCN* > 4 and ratio > 2	[27]

GCN, gene copy number; *AVGCN*, average gene copy number; *CNV*, copy number variation; *NAGK*, N-acetylglucosamine kinase

minimum), standard deviation, and variance regarding the parameters described below were calculated. Additionally, results were summarized in line and dot charts.

Results

Results of literature research

We conducted a systematic evaluation of previously published FISH criteria to detect *MYCN* amplification in RB and other tumor entities (detailed in Table 1). In total, 15 studies were included, which were published between 1995 and 2022. Only two publications were found with a primary focus on RB. Various approaches, including a great variety of calculated indices and cut-offs, were described. In summary, eight parameters were identified as potential measures of *MYCN* amplification in RB: average gene copy number (AVGCN) of *MYCN* signals/tumor cell, percent of tumor cells with a gene copy number (GCN) > 8, percent of tumor cells with GCN > 10, percent of tumor cells with cluster formation (defined as GCN of at least 15 per nucleus), average of target/reference ratio (*MYCN* signals/CEN2 signals), percent of tumor cells with target/reference ratio > 2, percent of tumor cells with target/reference ratio > 4, and difference between target (*MYCN*) and reference (CEN2) gene. The number of counted nuclei was between 50 and 200 in published studies.

Definition of FISH parameters based on analyses of the retrospective group

We applied the eight potential FISH parameters described above to the retrospective group of RB samples with known amplification to explore the distribution of measures and to discover parameters and thresholds, which allow doubtless identification of *MYCN* amplification. Additionally, the overall percentage of amplified areas, i.e., the proportion of tumor area, which is occupied by tumor cells with obvious cluster formation in relation to the total tumor area, was estimated.

We noticed that average target/reference ratio (*MYCN*/CEN2 ratio), target–reference difference (*MYCN*-CEN2; i.e. difference between average *MYCN* gene copy number and average CEN2 signals per cell), and AVGCN of *MYCN* per cell—in descending order—revealed the lowest standard deviation and variance (Table 2). Based on this finding, we

Table 2 MYCN FISH results of the retrospective group

Parameter	Range			Mean			Median			Standard deviation			Variance		
Cells	20	50	100	20	50	100	20	50	100	20	50	100	20	50	100
Target/reference ratio	57.8 (1.4–59.2)	47.4 (1.6–49)	25.7 (1.6–27.3)	14.44	13.86	11.76	7	8	7.9	16.85	13.76	8.51	283.79	189.37	72.44
MYCN-CEN2 difference	69.1 (0.7–69.8)	65.8 (1.4–67.2)	56.4 (1.5–57.9)	31.23	31.76	27.84	26.5	23.4	23.8	24.54	23.41	18.35	602.2	547.86	336.59
AVGCN	69.8 (2.7–72.5)	66.7 (3.9–70.6)	57.3 (3.9–61.2)	34.43	34.96	30.96	32.1	28.2	37.9	24.42	23.47	18.74	596.52	550.67	351.03
% of cells GCN > 8	100 (0–100)	100 (0–100)	100 (0–100)	78.18	78	77.91	59	52	52	39.32	34.34	29.19	1546.36	1179.2	852.09
% of cells GCN > 10	100 (0–100)	100 (0–100)	99 (0–99)	63.18	62	58.45	75	70	60	35.87	32.45	28.48	1286.36	1052.8	811.27
% of cells with *MYCN* clusters	100 (0–100)	100 (0–100)	99 (0–99)	61.82	62	57.09	75	70	60	34.81	32.45	27.89	1211.36	1052.8	778.09
% of cells with target/reference ratio > 2	85 (15–100)	58 (42–100)	80 (20–100)	74.09	73.36	75.45	85	80	82	31.05	23.31	24.83	964.091	543.26	616.27
% of cells with target/reference ratio > 4	100 (0–100)	100 (0–100)	100 (0–100)	63.18	60.64	66.09	65	62	66	38.68	32.15	29.79	1496.36	1033.7	887.69

Eight parameters obtained from systematic literature research were analyzed in eleven RB samples with known *MYCN* amplification. Range (minimum–maximum), mean, median, standard deviation, and variance regarding 20, 50, and 100 cells for all eight parameters are displayed. Target/reference ratio (*MYCN* signals/CEN2 signals), difference of *MYCN*-CEN2 gene copy number, and *MYCN* average gene copy number per cell (AVGCN) showed the lowest standard deviation and variance among all tested parameters. *GCN*, gene copy number. Raw data are displayed in supplementary Table SI2

recognized these three parameters as the most reliable to detect *MYCN* amplification. The percentage of amplified areas ranged between 40 and 90% (Supplemental material SI 2).

To define the minimum number of tumor cells, which need to be evaluated, all parameters were determined after 20, 50, and 100 counted cells (Table 2, supplemental material SI 2; Fig. 1). Due to intratumoral heterogeneity, values of parameters varied depending on how many cells were counted. For the preferred parameters, ten out of eleven samples (91%) could be identified as amplified if at least 50 tumor cells were analyzed and the following cut-offs were used: AVGCN ≥ 10, *MYCN*/CEN2 ratio ≥ 3, and *MYCN*-CEN2 difference ≥ 8. Counting only 20 tumor cells resulted in a lower detection rate.

Only one out of eleven RB samples, which were pretested to be *MYCN*-amplified by qPCR (ΔCT value: 17.69), was consistently negative for all parameters.

Application of FISH findings to a prospective RB group

Then, we analyzed an unselected series of an additional 33 clinical cases subsequently in the prospective group. We determined the following three parameters and cut-offs for 50 and 100 cells: *MYCN*/CEN2 ratio ≥ 3, AVGCN ≥ 10, and *MYCN*-CEN2 difference (*MYCN*-CEN2) ≥ 8 (Figs. 2 and 4 and supplemental information SI 3 and SI 4).

Four out of 33 cases were positive based on these three parameters/cut-offs. For these four cases, median AVGCN was 25.1 (range 17.9–41.9), median target/reference ratio was 13.4 (range 8.1–27.2), and median difference (*MYCN*-CEN2) was 23.2 (range 15.7–40.4). Consequently, the four cases were classified as *MYCN*-amplified. The remaining 29 cases were clearly below the set cut-offs and, therefore, were classified as negative for *MYCN* amplification. Median AVGCN was 2.3 (range 1.7–3.6), median target/reference ratio was 1.1 (range 0.9–1.4), and median difference (*MYCN*-CEN2) was 0.3 (range − 0.2–1.0) in these negative samples (supplemental information SI 3). Application of the three parameters mentioned above led to a prevalence of *MYCN* amplification in the prospective cohort of 12.1% (4/33).

Heterogeneity of FISH findings and correlation with morphology in amplified cases

Analysis of *MYCN*-amplified samples by FISH revealed that cluster formation can appear multifariously (Fig. 3). For example, clusters may impose diffusely tight and dust-like. Contrarily, clusters can be smaller and well defined with still increased counts of *MYCN* signals compared to CEN2 signals as reference. We observed polysomic samples where the count of both *MYCN* signals and

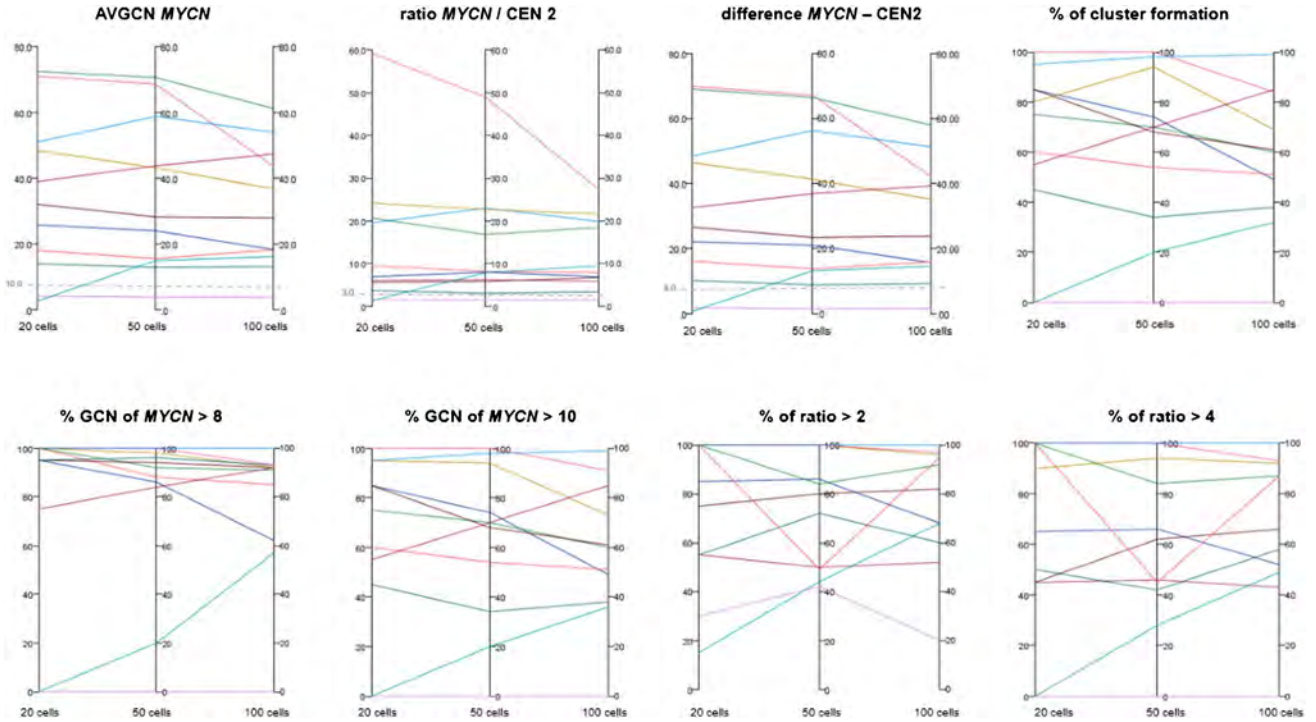

Fig. 1 Distribution of FISH parameters in the retrospective group of *MYCN*-amplified RB samples. Value ranges for 20, 50, and 100 tumor cells counted in the retrospective group of all eight parameters were examined. Each colored line represents one of eleven cases. Based on proposed cut-offs, i.e., AVGCN ≥ 10, *MYCN*/CEN2 ratio ≥ 3, and *MYCN*-CEN2 difference ≥ 8 (i.e. difference between average *MYCN* gene copy number and average CEN2 signals per cell), 10 samples could be identified as amplified if at least 50 tumor cells were analyzed. For a count of 20 cells, only nine of eleven cases revealed an AVGCN (*MYCN*) ≥ 10, an average target/reference ratio ≥ 3, and a difference between target and reference (*MYCN*-CEN2) ≥ 8. One case did not exceed cut-offs for 20, 50, and 100 cells (all tested parameters). Referring to a count of 20 cells, nine cases had cluster formation (min. to max 45–100%), gene copy number > 8% (75–100%), gene copy number > 10% (45–100%), and a ratio > 4 for a count of 20 cells (45–100%). For a count of 50 and 100 cells, ten cases showed cluster formation (20–98% for 50 cells and 32–99% for 100 cells), a gene copy number > 8% (20–100% for 50 cells and 57–100% for 100 cells), and a gene copy number > 10% (20–100% for 50 cells and 36–99% for 100 cells) (see also supplementary information SI 2). Nine cases reached a ratio > 4 for 50 and 100 cells, and eleven cases showed a ratio > 2 after counting 20 cells (15–100% of cells), 50 cells (42–100% of cells), and 100 cells (49–100% of cells). *AVGCN*, average gene copy number; *GCN*, gene copy number

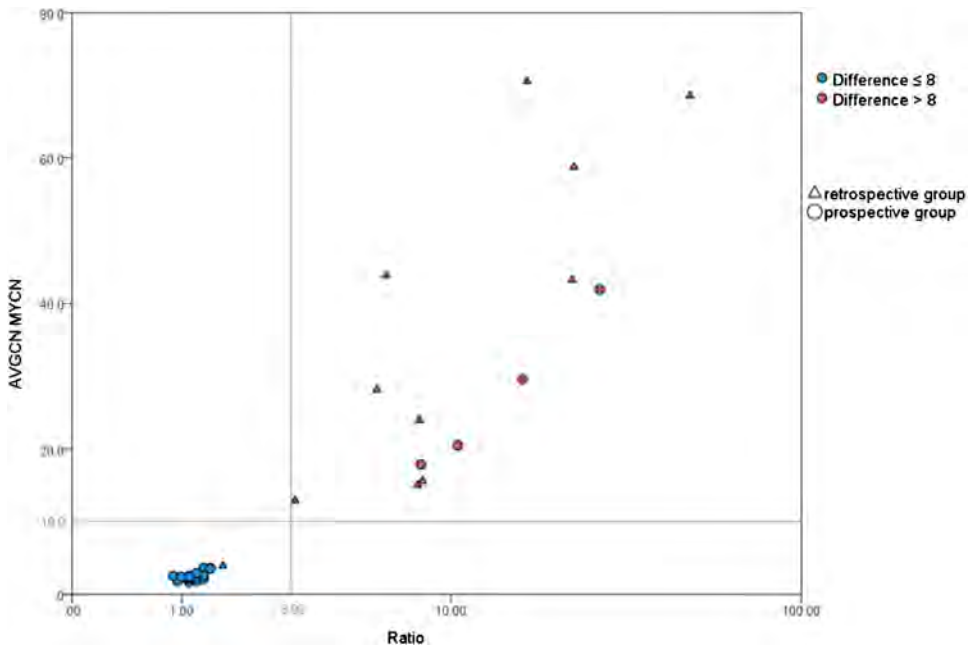

Fig. 2 Application of cut-offs to the retrospective and prospective group. Combined distribution of the three parameters chosen for all cases from the retrospective and prospective group referring to 50 counted cells. The cut-offs applied for ratio (≥ 3) and AVGCN (≥ 10) are each highlighted by a grey line. Four cases of the prospective and ten cases of the retrospective group each exceed all three cut-offs. One sample was close to cut-offs for ratio and AVGCN. In this sample, *MYCN*–CEN2 difference was > 8, which provided additional supporting evidence to classify this tumor as *MYCN*-amplified

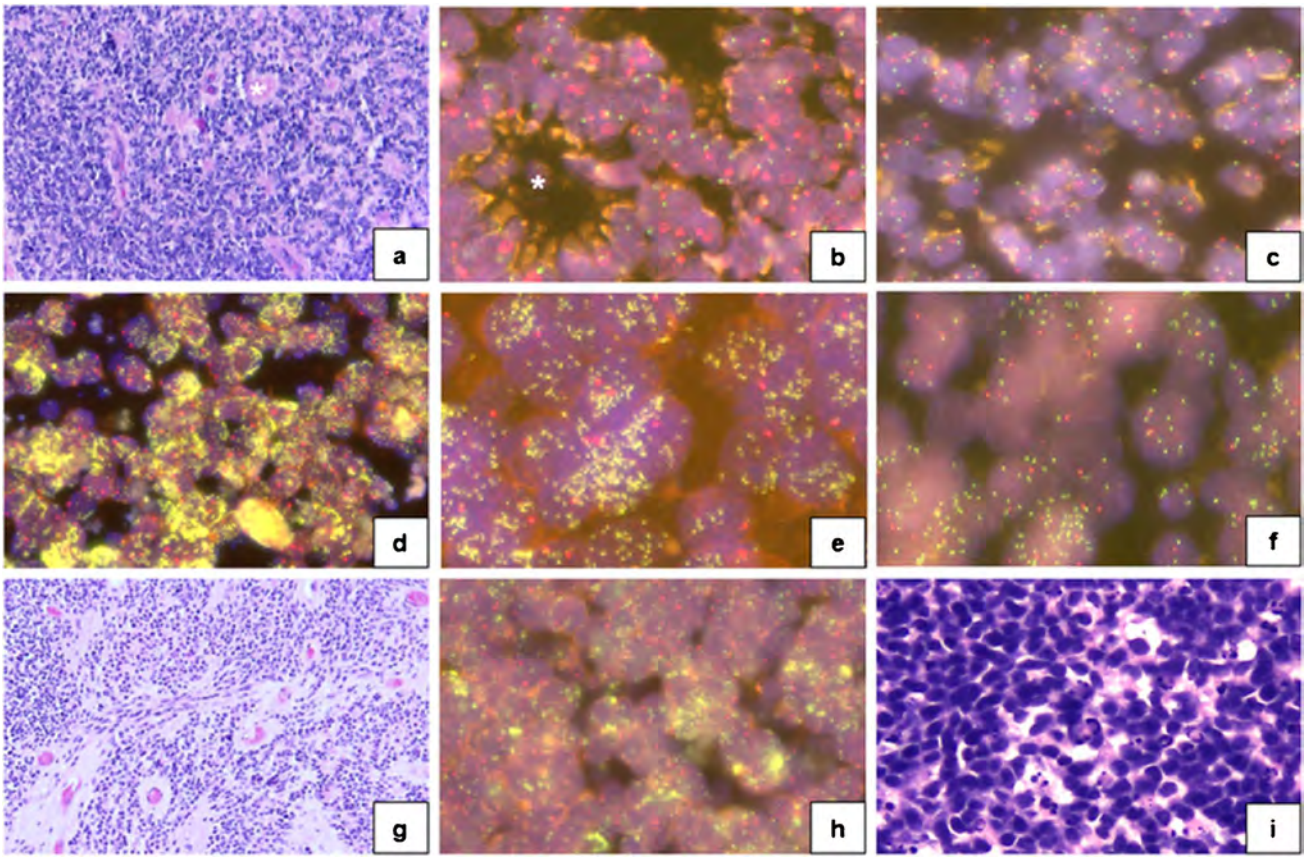

Fig. 3 Tumor morphology and FISH patterns. **a–c** H&E staining and FISH of non-amplified RB samples. **a** Abrupt transition between differentiated and undifferentiated morphology, namely small round and blue tumor cells with solid growth pattern and high cell density versus formation of Flexner-Winterstein rosettes (* indicates center of a rosette). **b** Eusomy (maximum of two green and two red signals per nucleus) and rosette formation. **c** Remarkable polysomy (> 2 green and orange signals per nucleus). **d–f** Different appearance of *MYCN* amplification in FISH. **d** Strong and diffuse cluster formation (green signals) with a dust-like appearance (fine and dense) so that the exact gene copy number of *MYCN* per cell can only be estimated (much more than 50 *MYCN* signals/cell). **e** Uniform and strong clear cluster formation of *MYCN* signals. **f** AVGCN around 10/nucleus; as CEN2 signal count is low (≤ 2/nucleus), the finding rather excludes polysomy as an explanation. **g–i** Intratumoral heterogeneity of *MYCN* amplification and mismatch with uniform undifferentiated HE morphology. **g** Undifferentiated morphology marked by high cell density, disordered solid growth pattern, and enlarged, hyperchromatic nuclei. **h** Heterogenously amplified tumor material with tight and dust-like cluster formation immediately adjacent to tumor cells with regular amount of green *MYCN* signals. **i** H&E staining of sample shown in **h** with uniform undifferentiated morphology, monomorphic small round and blue tumor cells and diffusely enlarged nuclei. Original magnifications: × 400 (H&E), × 630 (FISH)

CEN2 signals is increased. Moreover, *MYCN* amplification can be distributed heterogeneously with tight single-cell clusters next to tumor cells without any cluster formation. We noticed that tumor morphology, especially regarding differentiation of RB, was non-aligned with *MYCN* amplification status, as differentiated rosette-forming tumor areas did not show different FISH patterns than undifferentiated solid parts from the same tumor. Also, tumor areas with heterogeneously distributed cluster formations in FISH were found, which morphologically appeared as uniform undifferentiated tumors. Therefore, there was no correlation between tumor morphology and FISH findings.

Discussion

Standardized, clinically applicable FISH criteria are essential for detecting *MYCN* amplification, an emerging prognostic biomarker in retinoblastoma (RB). However, uniform definitions are lacking, and relevant studies remain limited. In this study, we first analyzed various published FISH criteria in a retrospective *MYCN*-amplified cohort ($n = 11$), including AVGCN of *MYCN*, target/reference signal ratios, cluster formation, and signal counts per nucleus. Most parameters reliably detected *MYCN* amplification, except for target/reference ratios > 2 or > 4, which proved either too unspecific or insufficiently sensitive.

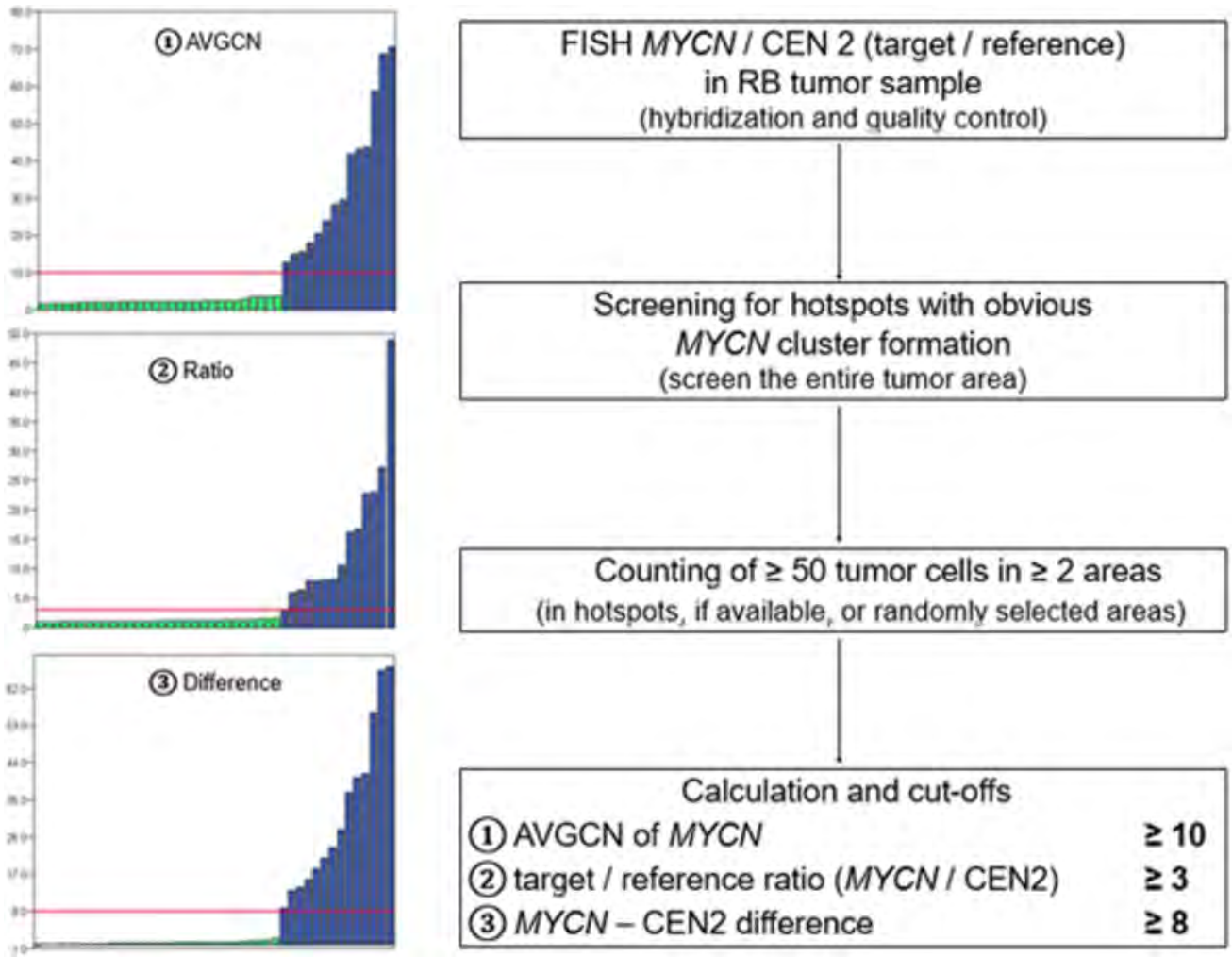

Fig. 4 Algorithm to evaluate *MYCN* amplification in RB. A four-step algorithm (right) summarizes the procedure how to evaluate, count, and calculate parameters of *MYCN* FISH in retinoblastomas. High average *MYCN* gene copy number per cell (AVGCN) and *MYCN*/CEN2 ratio define *MYCN*-amplified RB samples; *MYCN*–CEN2 difference (i.e. difference between average *MYCN* gene copy number and average CEN2 signals per cell) provides additional supporting evidence of amplification. Bar charts (left) demonstrate that MYCN-amplified cases are significantly above the thresholds

We selected the three most robust criteria—AVGCN ≥ 10, target/reference ratio ≥ 3, and *MYCN*–CEN2 difference ≥ 8—and applied them to a prospective cohort ($n = 33$). These consistently distinguished positive from negative cases, identifying four *MYCN*-amplified tumors. Our findings align with thresholds proposed by Misra et al. [41] and Santiago et al. [45] in RB and neuroblastoma, respectively. The *MYCN*-CEN2 difference criterion, previously used only in neuroblastoma by Wang et al. [48], also proved reliable.

Among the three parameters, AVGCN was the most discriminative. The ratio alone can be confounded by polysomy; however, when combined with AVGCN and difference, it enhanced diagnostic confidence. We recommend starting with AVGCN and ratio and applying the *MYCN*–CEN2 difference ≥ 8 in ambiguous cases (Fig. 4).

The optimal number of nuclei for FISH analysis remains debated. Literature reports vary from 50 to 200 cells. We found 50 nuclei sufficient, provided tumor sections are prescreened for cluster "hot spots" and evaluation includes at least two distinct areas. Intratumoral heterogeneity, as seen in one retrospective case, can lead to false negatives if sampling is insufficient.

Notably, one qPCR-positive retrospective case was FISH-negative, likely due to sampling discrepancies or heterogeneity. This underscores the need for cautious interpretation when discordant results arise. In general, Ct-values (qPCR) and numbers of *MYCN* gene copies (FISH) correlated

qualitatively to differentiate amplified from non-amplified cases; however, no linear correlation was observed.

While *MYCN* amplification is generally rare (reportedly in the range of 1–2% [7, 10, 12]), our prospective cohort showed a 12.1% prevalence, possibly due to analyzing enucleated, advanced-stage tumors. Given the limited data currently available on the prevalence of *MYCN* amplification in the literature, further investigation in this area is clearly warranted. To enable meaningful comparison across studies and ensure diagnostic accuracy, the establishment of standardized criteria for the reliable detection of *MYCN* amplification is essential. Since *MYCN*-amplified RB often presents more aggressively, targeted post-treatment surveillance in these cases is needed.

Our retrospective group also showed frequent co-occurrence of *MYCN* amplification and *RB1* mutations—contrary to earlier reports suggesting mutual exclusivity. All 11 *MYCN*-amplified tumors had *RB1* mutations, mostly biallelic, echoing findings from Ewens et al. [50] and Roohollahi et al. [12]. *RB1* data from 19 cases of the prospective cohort were available, and biallelic *RB1* loss was determined in 15/15 non-amplified and 3/4 amplified cases.

Limitations of this study include the relatively small sample size of both the prospective cohort ($n = 33$) and the retrospective cohort ($n = 11$). However, these numbers must be considered in the context of retinoblastoma being an ultra-rare pediatric malignancy, with an incidence of approximately 0.4 per 100,000 annually. Moreover, due to the widespread adoption of eye-preserving treatment strategies—now applied in over 70% of cases [1, 3]—histological evaluation is restricted to the minority of patients who undergo enucleation. This significantly limits access to tumor tissue suitable for molecular analyses. Our study included all available high-quality, matched fresh frozen and paraffin-embedded samples from our reference center. To our knowledge, no comparable dataset currently exists in Europe.

While we acknowledge the limited cohort size as a constraint, we emphasize the rarity and scientific value of this well-characterized material. Our findings provide a foundation for further research and suggest that *MYCN* FISH may be sufficient for clinical screening. Future studies should aim to validate this approach in larger, routinely collected diagnostic cohorts.

We believe our study offers a robust and specific assay that can contribute to the harmonization of *MYCN* testing in retinoblastoma and facilitate systematic investigation of this biomarker across centers.

Our data provide compelling evidence that *MYCN* FISH is a technically robust and reliable methodology, as all samples in our cohort (100%) were successfully evaluable without the need for repeat testing. Notably, the samples were obtained from multiple institutions, encompassing a range of local protocols for fixation and tissue processing. This underscores the broad applicability and resilience of the FISH technique across varying pre-analytical conditions.

However, certain fundamental technical requirements must be met to ensure optimal performance. Careful evaluation of internal controls is essential, particularly the signal distribution in non-neoplastic cells and the integrity of the centromeric control probe (CEN2). The presence of viable tumor tissue is critical; areas of necrosis and dystrophic calcification should be avoided, as these can compromise signal quality. In addition, decalcification procedures may adversely affect hybridization efficiency and should be minimized or carefully controlled. Proper grossing, section thickness, and adequate fixation are also key factors influencing assay success. When these pre-analytical and analytical considerations are addressed, FISH demonstrates an exceptionally low failure rate and high diagnostic reliability, as evidenced by the consistent success observed across our multi-institutional cohort.

FISH and Next-Generation Sequencing (NGS) are both widely used techniques for detecting gene amplification, each with distinct advantages and limitations. FISH enables the direct visualization of gene amplifications at the single-cell level within preserved tissue architecture, providing valuable spatial context and allowing detection of intratumoral heterogeneity. It is highly specific due to the use of fluorescently labeled probes targeting the gene of interest and performs reliably on formalin-fixed, paraffin-embedded (FFPE) tissue, which is standard in clinical pathology. Furthermore, FISH offers relatively fast turnaround times, is cost-effective for single-gene analysis, and is already clinically validated for multiple oncogenes, such as *HER2*.

In contrast, NGS provides high-throughput, genome-wide analysis, allowing for the simultaneous detection of amplifications, mutations, deletions, and other genomic alterations. It offers digital, quantitative assessment of copy number variations and is highly scalable, making it suitable for broader genomic profiling. However, NGS has several limitations: it requires high-quality DNA, which is often difficult to obtain from FFPE tissues; it lacks spatial resolution, meaning it cannot distinguish between tumor and non-tumor cells within a sample; and it involves complex and time-consuming data analysis, requiring robust bioinformatics infrastructure and expertise.

While NGS is a powerful tool for comprehensive genomic profiling, FISH holds clear advantages when the goal is focused, high-confidence detection of gene amplification—especially in rare cancers or small cohorts where tissue availability and preservation are critical concerns. Its robustness on FFPE samples, retention of histological context, and established clinical utility make FISH particularly well suited for routine diagnostics and retrospective studies.

This is the first study to systematically evaluate and validate FISH criteria for *MYCN* amplification in RB using a qPCR-confirmed control group. Our results support

implementation of standardized FISH protocols in clinical diagnostics. Although *MYCN* amplification is linked to poor prognosis, therapeutic implications remain undefined. As in medulloblastoma, where FISH is the gold standard, these criteria may also prove useful in other tumor types, warranting further investigation.

In summary, our proposed FISH criteria offer a reliable and practical approach for identifying *MYCN*-amplified RB, supporting personalized aftercare strategies in affected children post-enucleation.

Supplementary Information The online version contains supplementary material available at https://doi.org/10.1007/s00428-025-04219-x.

Acknowledgements The authors are grateful to D. R. Lohmann and D. Kanber, Institute of Human Genetics and Eye Oncogenetics Research Group, University Hospital Essen, University of Duisburg-Essen, Essen, Germany, for providing qPCR data.

Author contribution Conceptualization: CB, HUS, ST; data curation: CB, TH, NS, HUS, ST; formal analysis: CB; funding acquisition: PK; investigation and methodology: CB, TH, NS, HUS, ST; project administration: HUS, ST; resources: PK, EB, TK, KP, PT, MB, JR, HUS; software: not applicable; supervision: HUS, ST; validation: CB, HUS, ST; visualization: CB; writing—original draft: CB, HUS; writing—review and editing: all authors.

Funding This research was funded by "Deutsche Kinderkrebsstiftung" (Grant no. DKS2020.14 and DKS2024.08).

Data availability Raw data is available in supplemental files.

Declarations

Ethical approval This study has been approved by local ethics committees: 13–5405-BO [12/04/2023], Ethik-Kommission der Medizinischen Fakultät der Universität Duisburg-Essen, and 2024–3926-evBO [FF61/2014], Ethik-Kommission bei der Landesärztekammer Hessen.

Conflict of interest HUS is an employee of Discovery Life Sciences; honoraria for advisory board memberships, research support, and reimbursements from Daiichi Sankyo, AstraZeneca, BMS, Astellas, Zytomed Systems, ZytoVision, MSD, Merck, Agilent, and Roche have been paid to the employer. All remaining authors declare no conflict of interest.

References

1. Stacey AW, Bowman R, Foster A, Kivelä TT, Munier FL, Cassoux N, Fabian ID, Global Retinoblastoma Study Group (2021) Incidence of retinoblastoma has increased: results from 40 European countries. Ophthalmology 128(9):1369–1371. https://doi.org/10.1016/j.ophtha.2021.01.024
2. Global Retinoblastoma Study Group (2022) The global retinoblastoma outcome study: a prospective, cluster-based analysis of 4064 patients from 149 countries. Lancet Glob Health 10(8):e1128–e1140. https://doi.org/10.1016/S2214-109X(22)00250-9
3. Lavasidis G, Papaioannou K, Anagnostou N, Ketteler P, Bechrakis NE, Ntzani E (2024) Evidence in focus: the sparse landscape of randomized trials on retinoblastoma. Treat Ocul Oncol Pathol 10(1):53–62. https://doi.org/10.1159/000536410
4. Kaliki S, Vempuluru VS, Fabian ID, Abdallah E, Abdullahi SU, Abdulqader RA, Abdulrahaman AA, Abouelnaga S, Ademola-Popoola DS, Adio A, Afifi MA (2025) Retinoblastoma with and without extraocular tumor extension: a global comparative study of 3435 patients. Ophthalmol Sci 5(2):100637. https://doi.org/10.1016/j.xops.2024.100637
5. Rating P, Bornfeld N, Schlüter S, Westekemper H, Kiefer T, Stuschke M, Göricke S, Ketteler P, Ting S, Metz KA, Bechrakis NE, Biewald E (2022) Long-term results after intraocular surgery in treated retinoblastoma eyes. Ocul Oncol Pathol 8(3):161–167. https://doi.org/10.1159/000524610
6. Knudson AG Jr (1971) Mutation and cancer: statistical study of retinoblastoma. Proc Natl Acad Sci U S A 68(4):820–823. https://doi.org/10.1073/pnas.68.4.820
7. Lohmann DR, Gallie BL (2000) Retinoblastoma. [Updated 2023 Sep 21]. In: Adam MP, Feldman J, Mirzaa GM et al (eds) GeneReviews®. University of Washington, Seattle. Available from: https://www.ncbi.nlm.nih.gov/books/NBK1452/
8. Kooi IE, Mol BM, Moll AC, van der Valk P, de Jong MC, de Graaf P, van Mil SE, Schouten-van Meeteren AY, Meijers-Heijboer H, Kaspers GL, Te Riele H, Cloos J, Dorsman JC (2015) Loss of photoreceptorness and gain of genomic alterations in retinoblastoma reveal tumor progression. EBioMedicine 2(7):660–670. https://doi.org/10.1016/j.ebiom.2015.06.022
9. Ryl T, Afanasyeva E, Hartmann T et al (2024) A *MYCN*-driven de-differentiation profile identifies a subgroup of aggressive retinoblastoma. Commun Biol 7(1):919. https://doi.org/10.1038/s42003-024-06596-6
10. Rushlow DE, Mol BM, Kennett JY et al (2013) Characterisation of retinoblastomas without *RB1* mutations: genomic, gene expression, and clinical studies. Lancet Oncol 14(4):327–334. https://doi.org/10.1016/S1470-2045(13)70045-7
11. Liu J, Ottaviani D, Sefta M et al (2021) A high-risk retinoblastoma subtype with stemness features, dedifferentiated cone states and neuronal/ganglion cell gene expression. Nat Commun 12(1):5578. https://doi.org/10.1038/s41467-021-25792-0
12. Roohollahi K, de Jong Y, van Mil SE, Fabius AWM, Moll AC, Dorsman JC (2022) High-level *MYCN*-amplified *RB1*-proficient retinoblastoma tumors retain distinct molecular signatures. Ophthalmol Sci 2(3):100188. https://doi.org/10.1016/j.xops.2022.100188
13. Li WL, Buckley J, Sanchez-Lara PA, Maglinte DT, Viduetsky L, Tatarinova TV, Aparicio JG, Kim JW, Au M, Ostrow D, Lee TC, O'Gorman M, Judkins A, Cobrinik D, Triche TJ (2016) A rapid and sensitive next-generation sequencing method to detect *RB1* mutations improves care for retinoblastoma patients and their families. J Mol Diagn. https://doi.org/10.1016/j.jmoldx.2016.02.006
14. de Bloeme CM, Jansen RW, Cardoen L, Göricke S, van Elst S, Jessen JL, Ramasubramanian A, Skalet AH, Miller AK, Maeder P, Uner OE (2024) Differentiating MYCN-amplified

RB1 wild-type retinoblastoma from biallelic RB1 mutant retinoblastoma using MR-based radiomics: a retrospective multicenter case–control study. Sci Rep 14(1):25103. https://doi.org/10.1038/s41598-024-76933-6
15. Zugbi S, Ganiewich D, Bhattacharyya A, Aschero R, Ottaviani D, Sampor C, Cafferata EG, Mena M, Sgroi M, Winter U, Lamas G (2020) Clinical, genomic, and pharmacological study of *MYCN*-amplified *RB1* wild-type metastatic retinoblastoma. Cancers (Basel) 12(9):2714. https://doi.org/10.3390/cancers12092714
16. Stenfelt S, Blixt MKE, All-Ericsson C, Hallböök F, Boije H (2017) Heterogeneity in retinoblastoma: a tale of molecules and models. Clin Transl Med 6(1):42. https://doi.org/10.1186/s40169-017-0173-2
17. Shapiro DN, Valentine MB, Rowe ST, Sinclair AE, Sublett JE, Roberts WM, Look AT (1993) Detection of N-myc gene amplification by fluorescence in situ hybridization. Diagnostic utility for neuroblastoma. Am J Pathol 142(5):1339
18. Malakho SG, Korshunov A, Stroganova AM, Poltaraus AB (2008) Fast detection of *MYCN* copy number alterations in brain neuronal tumors by real-time PCR. J Clin Lab Anal 22(2):123–130. https://doi.org/10.1002/jcla.20232
19. Ruiz-Pérez MV, Henley AB, Arsenian-Henriksson M (2017) The MYCN protein in health and disease. Genes 8(4):113. https://doi.org/10.3390/genes8040113
20. Ghasemi DR, Sill M, Okonechnikov K et al (2019) *MYCN* amplification drives an aggressive form of spinal ependymoma. Acta Neuropathol 138(6):1075–1089. https://doi.org/10.1007/s00401-019-02056-2
21. Huang C, Jiang S, Yang J, Liao X, Li Y, Li S (2020) Therapeutic potential of targeting *MYCN*: a case series report of neuroblastoma with *MYCN* amplification. Medicine (Baltimore) 99(25):e20853. https://doi.org/10.1097/MD.0000000000020853
22. Hong B, Chen Z, Coffin CM, Lemons R, Issa B, Brothman A, Zhou H (2003) Molecular cytogenetic analysis of a pleuropulmonary blastoma. Cancer Genet Cytogenet 142(1):65–69. https://doi.org/10.1016/s0165-4608(02)00731-8
23. Moreno DA, da Silva LS, Zanon MF et al (2022) Single nCounter assay for prediction of *MYCN* amplification and molecular classification of medulloblastomas: a multicentric study. J Neurooncol 157(1):27–35. https://doi.org/10.1007/s11060-022-03965-1
24. Williams RD, Al-Saadi R, Chagtai T, Popov S, Messahel B, Sebire N, Gessler M, Wegert J, Graf N, Leuschner I, Hubank M, Jones C, Vujanic G, Pritchard-Jones K, Children's Cancer and Leukaemia Group, SIOP Wilms' Tumour Biology Group (2010) Subtype-specific *FBXW7* mutation and *MYCN* copy number gain in Wilms' tumor. Clin Cancer Res 16(7):2036–2045. https://doi.org/10.1158/1078-0432.CCR-09-2890
25. Nessling M, Solinas-Toldo S, Wilgenbus KK, Borchard F, Lichter P (1998) Mapping of chromosomal imbalances in gastric adenocarcinoma revealed amplified protooncogenes MYCN, MET, WNT2, and ERBB2. Genes Chromosomes Cancer 23(4):307–316. https://doi.org/10.1002/(sici)1098-2264(199812)23:4<307::aid-gcc5>3.0.co;2-#
26. Beltran H, Rickman DS, Park K, Chae SS, Sboner A, MacDonald TY, Wang Y, Sheikh KL, Terry S, Tagawa ST, Dhir R, Nelson JB, de la Taille A, Allory Y, Gerstein MB, Perner S, Pienta KJ, Chinnaiyan AM, Wang Y, Collins CC, Gleave ME, Demichelis F, Nanus DM, Rubin MA (2011) Molecular characterization of neuroendocrine prostate cancer and identification of new drug targets. Cancer Discov 1(6):487–495. https://doi.org/10.1158/2159-8290.CD-11-0130
27. Mosquera JM, Beltran H, Park K, MacDonald TY, Robinson BD, Tagawa ST, Perner S, Bismar TA, Erbersdobler A, Dhir R, Nelson JB, Nanus DM, Rubin MA (2013) Concurrent *AURKA* and *MYCN* gene amplifications are harbingers of lethal treatment-related neuroendocrine prostate cancer. Neoplasia 15(1):1–10. https://doi.org/10.1593/neo.121550
28. Goto S, Umehara S, Gerbing RB, Stram DO, Brodeur GM, Seeger RC, Lukens JN, Matthay KK, Shimada H (2001) Histopathology (International Neuroblastoma Pathology Classification) and *MYCN* status in patients with peripheral neuroblastic tumors: a report from the Children's Cancer Group. Cancer 92(10):2699–2708. https://doi.org/10.1002/1097-0142(20011115)92:10/3c2699::aid-cncr1624/3e3.0.co;2-a
29. Lee K, Kim SI, Kim EE, Shim YM, Won JK, Park CK, Choi SH, Yun H, Lee H, Park SH (2023) Genomic profiles of *IDH*-mutant gliomas: *MYCN*-amplified *IDH*-mutant astrocytoma had the worst prognosis. Sci Rep 13(1):6761. https://doi.org/10.1038/s41598-023-32153-y
30. Pfister S, Remke M, Benner A, Mendrzyk F, Toedt G, Felsberg J, Wittmann A, Devens F, Gerber NU, Joos S, Kulozik A, Reifenberger G, Rutkowski S, Wiestler OD, Radlwimmer B, Scheurlen W, Lichter P, Korshunov A (2009) Outcome prediction in pediatric medulloblastoma based on DNA copy-number aberrations of chromosomes 6q and 17q and the *MYC* and *MYCN* loci. J Clin Oncol 27(10):1627–1636. https://doi.org/10.1200/JCO.2008.17.9432
31. Bourdeaut F, Grison C, Maurage CA, Laquerriere A, Vasiljevic A, Delisle MB, Michalak S, Figarella-Branger D, Doz F, Richer W, Pierron G, Miquel C, Delattre O, Couturier J (2013) *MYC* and *MYCN* amplification can be reliably assessed by aCGH in medulloblastoma. Cancer Genet 206(4):124–129. https://doi.org/10.1016/j.cancergen.2013.02.003
32. Overbeck TR, Cron DA, Schmitz K et al (2020) Top-level *MET* gene copy number gain defines a subtype of poorly differentiated pulmonary adenocarcinomas with poor prognosis. Transl Lung Cancer Res 9:603–616. https://doi.org/10.21037/tlcr-19-339
33. Schmitz K, Koeppen H, Binot E et al (2015) *MET* gene copy number alterations and expression of MET and hepatocyte growth factor are potential biomarkers in angiosarcomas and undifferentiated pleomorphic sarcomas. PLoS ONE 10:e0120079. https://doi.org/10.1371/journal.pone.012007
34. Schildhaus H-U, Heukamp LC, Merkelbach-Bruse S et al (2012) Definition of a fluorescence in-situ hybridization score identifies high- and low-level *FGFR1* amplification types in squamous cell lung cancer. Mod Pathol 25:1473–1480. https://doi.org/10.1038/modpathol.2012.102
35. Mentzel T, Schildhaus HU, Palmedo G et al (2012) Postradiation cutaneous angiosarcoma after treatment of breast carcinoma is characterized by *MYC* amplification in contrast to atypical vascular lesions after radiotherapy and control cases: clinicopathological, immunohistochemical and molecular analysis of 66 cases. Mod Pathol 25:75–85. https://doi.org/10.1038/modpathol.2011.134
36. Schultheis AM, Bos M, Schmitz K et al (2014) Fibroblast growth factor receptor 1 (*FGFR1*) amplification is a potential therapeutic target in small-cell lung cancer. Mod Pathol 27:214–221. https://doi.org/10.1038/modpathol.2013.141
37. Stoss OC, Scheel A, Nagelmeier I et al (2015) Impact of updated HER2 testing guidelines in breast cancer–re-evaluation of HERA trial fluorescence in situ hybridization data. Mod Pathol 28:1528–1534. https://doi.org/10.1038/modpathol.2015.112
38. Rüschoff J, Nagelmeier I, Baretton G, Dietel M, Höfler H, Schildhaus HU, Büttner R, Schlake W, Stoss O, Kreipe HH (2010) Her2 testing in gastric cancer. What is different in comparison to breast cancer? Pathologe 31(3):208–17. https://doi.org/10.1007/s00292-010-1278-1
39. Schildhaus H-U, Schroeder L, Merkelbach-Bruse S et al (2013) Therapeutic strategies in male breast cancer: clinical implications of chromosome 17 gene alterations and molecular subtypes. Breast 22:1066–1071. https://doi.org/10.1016/j.breast.2013.08.008

40. Schildhaus H-U, Schultheis AM, Rüschoff J et al (2015) *MET* amplification status in therapy-naïve adeno- and squamous cell carcinomas of the lung. Clin Cancer Res 21:907–915. https://doi.org/10.1158/1078-0432.CCR-14-0450
41. Misra DN, Dickman PS, Yunis EJ (1995) Fluorescence in situ hybridization (FISH) detection of *MYCN* oncogene amplification in neuroblastoma using paraffin-embedded tissues. Diagn Mol Pathol 4(2):128–135. https://doi.org/10.1097/00019606-199506000-00009
42. Raffeld M, Abdullaev Z, Pack SD, Xi L, Nagaraj S, Briceno N, Vera E, Pittaluga S, Lopes Abath Neto O, Quezado M, Aldape K, Armstrong TS, Gilbert MR (2020) High level *MYCN* amplification and distinct methylation signature define an aggressive subtype of spinal cord ependymoma. Acta Neuropathol Commun 8(1):101. https://doi.org/10.1186/s40478-020-00973-y
43. Scheil S, Brüderlein S, Eicker M, Herms J, Herold-Mende C, Steiner HH, Barth TF, Möller P (2001) Low frequency of chromosomal imbalances in anaplastic ependymomas as detected by comparative genomic hybridization. Brain Pathol 11(2):133–143. https://doi.org/10.1111/j.1750-3639.2001.tb00386.x
44. Hong L, Shi ZF, Li KK, Wang WW, Yang RR, Kwan JS, Chen H, Li FC, Liu XZ, Chan DT, Li WC, Zhang ZY, Mao Y, Ng HK (2022) Molecular landscape of pediatric type *IDH* wildtype, *H3* wildtype hemispheric glioblastomas. Lab Invest 102(7):731–740. https://doi.org/10.1038/s41374-022-00769-9
45. Santiago T, Tarek N, Boulos F, Hayes C, Jeha S, Raimondi S, Rodriguez-Galindo C (2019) Correlation between *MYCN* gene status and MYCN protein expression in neuroblastoma: a pilot study to propose the use of MYCN immunohistochemistry in limited-resource areas. J Glob Oncol 5:1–7. https://doi.org/10.1200/JGO.19.00135
46. Zimling ZG, Rechnitzer C, Rasmussen M, Petersen BL (2007) Peripheral neuroblastic tumours in eastern Denmark 1972–2002. APMIS 115(1):66–74. https://doi.org/10.1111/j.1600-0463.2007.apm_355.x
47. Su Y, Wang L, Zhao Q, Yue Z, Zhao W, Wang X, Duan C, Jin M, Zhang D, Chen S, Yin J (2020) Implementation of the plasma *MYCN*/*NAGK* ratio to detect *MYCN* amplification in patients with neuroblastoma. Mol Oncol 14(11):2884–93. https://doi.org/10.1002/1878-0261.12794
48. Wang M, Zhou C, Cai R, Li Y, Gong L (2013) Copy number gain of *MYCN* gene is a recurrent genetic aberration and favorable prognostic factor in Chinese pediatric neuroblastoma patients. Diagn Pathol 8:5. https://doi.org/10.1186/1746-1596-8-5
49. Ting SC, Kiefer T, Ehlert K, Goericke SL, Hinze R, Ketteler P, Bechrakis NE, Schildhaus HU (2020) Bone metastasis of retinoblastoma five years after primary treatment. Am J Ophthalmol Case Rep 19:100834. https://doi.org/10.1016/j.ajoc.2020.100834
50. Ewens KG, Bhatti TR, Moran KA, Richards-Yutz J, Shields CL, Eagle RC, Ganguly A (2017) Phosphorylation of pRb: mechanism for RB pathway inactivation in *MYCN*-amplified retinoblastoma. Cancer Med 6(3):619–630. https://doi.org/10.1002/cam4.1010